

1.09 HEAT TRANSPORT SIMULATIONS IN A QUASI TWO-DIMENSIONAL WAKE INTERACTING WITH A BOUNDARY LAYER USING THE LAGRANGIAN PARTICLE DISPERSION MODEL DIPCOT.

Efstratios Davakis¹, Spyros Andronopoulos², George A. Sideridis¹, Eleftherios G. Kastrinakis¹, John G. Bartzis³, Stavros G. Nychas¹

¹Department of Chemical Engineering, Aristotle University of Thessaloniki, Greece,

²Environmental Research Laboratory, Institute of Nuclear Technology and Radiation Protection, NCSR "Demokritos", Greece, ³Department of Energy Resources Management Engineering, Aristotle University of Thessaloniki, Greece.

INTRODUCTION

The Lagrangian particle dispersion model DIPCOT was applied in order to perform heat transport simulations, using data from a wind tunnel experiment where quasi two-dimensional flow was produced by the interaction of wake behind a cylinder and a turbulent boundary layer. Heat was supplied to the boundary layer by means of a line heat source. Heat dispersion simulations were performed and the temperature rise was computed. The calculated temperatures were statistically and qualitatively compared with the experimental ones. Power spectrum analysis was also performed for temperature in order to examine possible deviations from the $-5/3$ power law and the degree of agreement between the experimental and the predicted concentrations. Comparisons between the estimated Lagrangian probability density function and the Eulerian one were also conducted at predefined locations.

The profiles of the calculated temperatures are very close to the experimental ones especially inside the boundary layer. The model experiences some difficulties over the boundary layer; however, the mean behavior of the model over space and time is quite satisfactory. The power spectra density of both predicted and experimental temperatures deviate from the $-5/3$ power law, but there is difference between them concerning the number of the regions with different slopes and the range of each region.

EXPERIMENTAL SETUP AND LABORATORY DATA

In order to examine the structure of such flows a cylinder was placed parallel to a flat plate and normal to the flow (*Sideridis G.A., et al* 1998, 1999 and 2002). The cylinder was positioned above the boundary layer, so that the lower part of the wake was interacting with the boundary layer. Heat was supplied to the boundary layer flow by means of an (1.85 m long) electrically heated wire (19 Volt, 520 mA at the edges). Since the Prandtl and Schmidt numbers are both close to unity for gases and the heat dispersion exhibits the same features as the mass dispersion, this study is considered equivalent to atmospheric dispersion over complex terrain. The experiment was conducted in an open return, suction type wind tunnel (Figure 1). Hot-wire anemometry was used for the measurements with a triple-wire probe. During the experiment, the triple-wire probe recorded simultaneously the stream-wise and the normal velocity components and temperature every 0.25 ms during a time period of 12.5 sec. The probe was traversed normal to the plate, from $z=93$ mm to $z=4$ mm taking measurements at 41 observation heights, at the five measuring distances in the stream-wise direction: $x/D = 15, 20, 25, 30$ and 35 (D is the cylinder diameter). A schematic representation of the flow field is given in Figure 2.

THE MODEL DESCRIPTION

The DIPCOT (e.g. *Davakis et. all*, 2004) is 3-dimensional Lagrangian particle dispersion model. The mass of a pollutant (heat in the present work) is distributed to a certain number of fictitious particles, which are displaced within the computational domain. The trajectory of each particle is estimated based on the mean wind velocity and the Langevin equation (*Thomson, D.J.*, 1987): $dx_i(t) = (\overline{U}_i + u'_i)\Delta t$ and $du'_i(t) = a_i dt + \sqrt{C_o \varepsilon(z)} dW_i$, where \overline{U}_i is the mean wind velocity in the three directions ($i=x,y,z$), u'_i is the turbulent particle velocity, dt is the time interval, C_o is a universal constant ($=3$ for the present study), $\varepsilon(z)$ is the ensemble-average rate of dissipation of turbulent kinetic energy and dW_i are increments of a Wiener process with zero mean and variance dt .

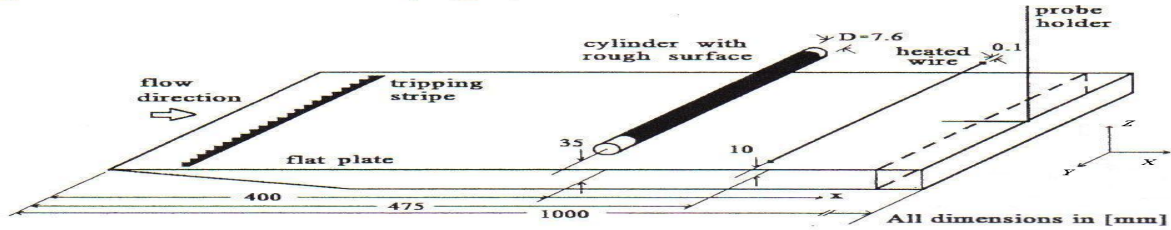


Figure 1. The experimental setup.

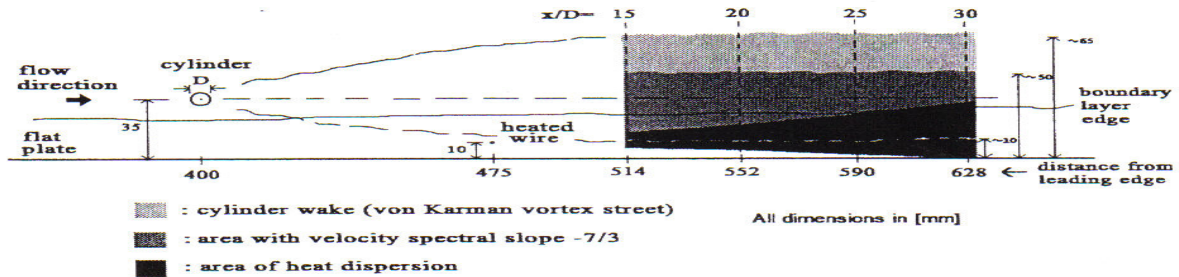


Figure 2. Schematic representation of the experimental flow created in the wind tunnel.

The deterministic acceleration term α_i is a function of turbulence statistics, which is derived using the “well mixed condition”, proposed by *Thomson, D.J.* (1987) from the Fokker-Plank equation. Assuming Gaussian homogeneous turbulence for the horizontal plane (*Wilson J.D. et al*, 1996) $\alpha_{x,y} = -C_o \varepsilon u'_{x,y} / 2\sigma_{x,y}^2$ and inhomogeneous skewed turbulence for the vertical direction (*Franzese P. et. al*, 1999) $\alpha_z = c_1(z)u'_z{}^2 + c_2(z)u'_z + c_3(z)$ where σ_i is the variance of the wind velocity fluctuations. The coefficients c_1 , c_2 and c_3 are height depended functions of the Eulerian vertical velocity moments (variance, skewness and flatness) and of their derivatives. In this paper the dissipation rate is computed based on the relations proposed by *Rodean, C.H.* (1994) $\varepsilon k / u_*^3 = (1/z)[1 + 3.7(z/L)](1 - 0.85z/h)^{3/2}$ where $k=0.04$ is the von Karman constant and L is the Monin–Obukhov length. The point high-frequency measurements of the instantaneous values of two velocity components were used to drive the mean wind profiles along with parameters such as variance, skewness and flatness of turbulent fluctuations. The line source was divided to 185-point sources and the total heat released from the wire was equally distributed in each point source. From each source 50000 particles were released during a time period of 12.5 sec. “Heat concentrations” were estimated in all the observation points for all the experimental time steps, using the box counting method (with dimensions $0.019 \times 0.070 \times 0.003 \text{ mm}^3$). The temperature rise (ΔT) was computed using the estimated heat concentration: $\Delta T = Q / (\rho C_p) \text{ } ^\circ\text{K}$, where Q is the “heat concentration” KJ/m^3 , C_p and ρ are the specific heat and density of air in $\text{KJ (Kg } ^\circ\text{K)}^{-1}$ and Kg/m^3 ,

respectively. The simultaneous temperatures are then estimated by adding the ambient atmospheric temperature ($T_o \sim 20$ °C): $T = T_o + \Delta T$.

RESULTS

The statistical evaluation of the model was performed using well-known statistical indices (e.g. Davakis, E., et al, 2004) such as the Fractional Bias (FB), the Geometric Mean bias (MG) the Normalized Mean Square Error (NMSE), the Geometric Variance (VG), the FACTor of two (FACT2), the FACTor of five (FACT5) and the Factor Of Exceedance (FOEX). The statistical analysis was carried out using the pairs of predicted and measured temperature rise (ΔT). The results of the analysis are presented in Table 1. The values of FB and MG, which are close to zero and unit, respectively and the relative high values of FACT2 and FACT5, indicate that the model overall behaves well. The model exhibits a small tendency towards overprediction for both higher and lower temperatures (FB less than zero and MG less than one), which is also pronounced by the positive value of FOEX. The values of NMSE and VG denote also small deviations from the observed temperatures.

Table 1. Statistical indices of comparison

Statistical Index	FB	NMSE	MG	VG	FACT2	FACT5	FOEX
	-0.28	0.6073	0.9449	4.0942	68.29	87.80	16.34

Comparisons between the mean experimental normalized temperature profiles ($\langle T \rangle / T_o$) and the estimated ones are presented in Figure 3a-d for all the downwind measuring distances. The normalized temperatures are plotted against normalized distance from plate Z^+ ($=u_* z/v$, where $v=1.465 \times 10^{-5}$ m²/s is the kinematic viscosity of air). The results of the statistical analysis can be observed in Figure 2, where the mean normalized temperature profiles are displayed. As it can be seen in Figure 3a-b, near the line source, where the heat dispersion is quite small the model predictions are almost perfected. The simulated dispersion experience the most difficulties over the boundary layer ($Z^+=260$), where the estimated mean temperatures are over-predicted, indicating smaller spread of heat (Figure 3c-e). However, the model simulations under the boundary layer height remain quite satisfactory.

The Lagrangian PDF, which is a numerical approximation to the Eulerian wind velocity PDF, can be computed by sampling the particle velocity field at various locations. Figure 4a-d compare the vertical particle velocity PDFs, for two measuring downwind distance ($x/D=20$ and 30), with the Eulerian ones. The comparison was made at two levels at each x/D . The first level was near the line source height at $Z^+=132$ and the second near the boundary layer height at $Z^+=262$. The Lagrangian particle PDF is very close to the Eulerian PDF near the line source height (Figure 4a and c) at the lower part of the dispersion area. The particle velocity distribution follows the distribution of the wind velocity fluctuations. There are small differences in the peak values (small underestimation) and at the magnitude of the higher fluctuations. However, the deviations increase with height (Figure 4b and 4d). The mode of the PDF is underestimated at higher altitudes. The width and the peaks of the Lagrangian PDFs are smaller than the Eulerian. This is in agreement with the above-mentioned overestimations of the predicted temperatures. The particle spread throughout the computational domain is limited by the lower values of the simulated fluctuations and consequently heat dispersion is underestimated resulting in greater temperature calculation.

Power spectrum analysis was performed for temperature using the time series of the predicted and the observed temperatures. Power Spectra Density (PSD) plots of the vertical velocity are presented. The PSD of the experimental concentrations at $x/D=20$ and $Z^+=132$ and 262

(Figure 5a1-a2) presents a scaling region with a slope $-5/3$, extending approximately from 50 to 150 Hz, followed by a region with slope $-7/3$ (150-400 Hz) and successively from other two regions with slopes greater than $-7/3$ and smaller than $-5/4$, respectively. Model simulation shows similar behavior (Figure 5b1-b2). There are also two regions with slopes $-5/3$ and $-7/3$. However, the range is not the same (150-300 and 300-700 Hz respectively for the two slops). Moreover only one other major region exists with slope less than $-5/3$.

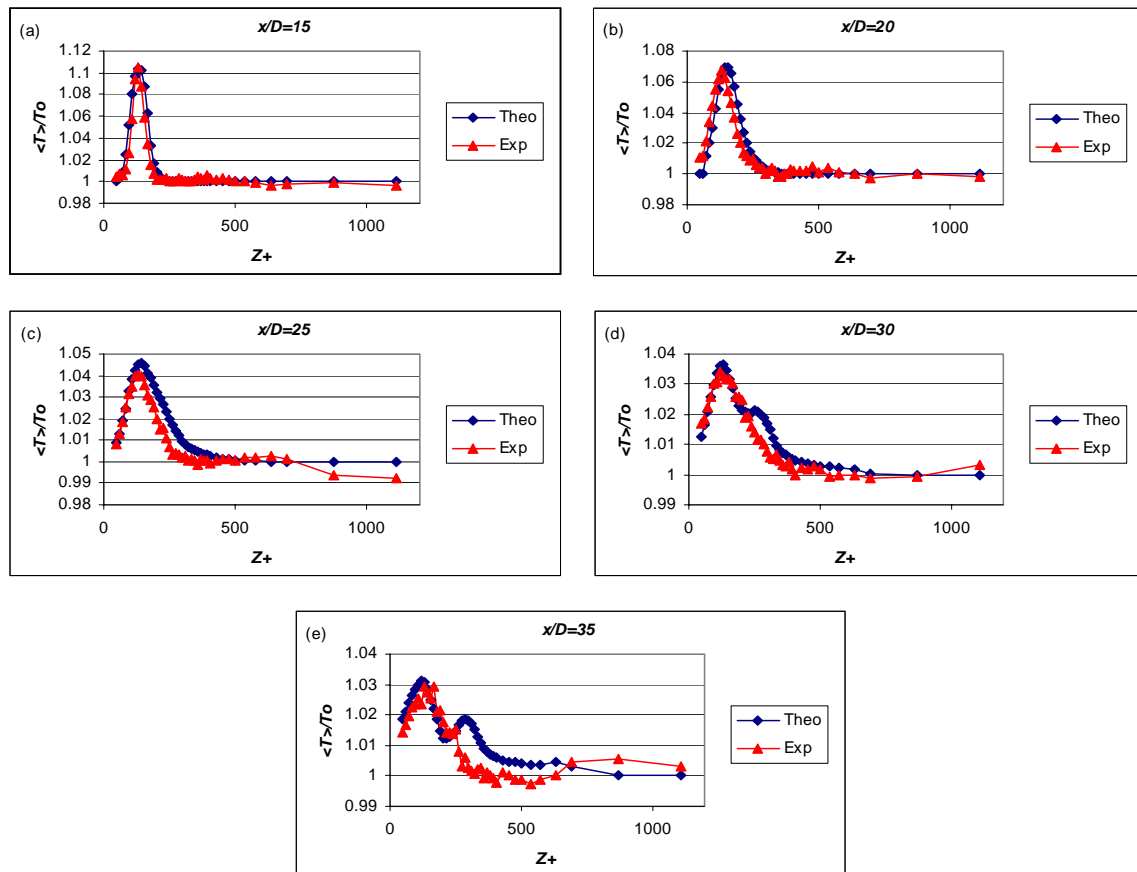


Figure 3. Mean normalized experimental and theoretical temperature profiles for all the downwind measuring distances ($x/D=15, 20, 25, 30, 35$)

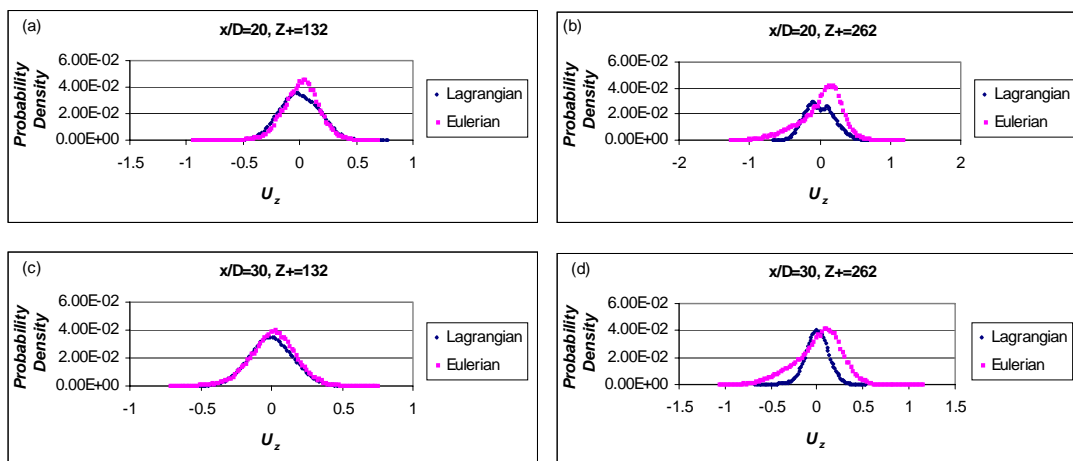


Figure 4. Probability density functions of experimental (Eulerian) and predicted vertical velocity distributions at $x/D=20$ and normalized heights $Z_+=132$ (a), 262 (b)

CONCLUSIONS

The overall performance of the model can be characterized as satisfactory, taking into consideration the complexity of the flow. The statistical analysis showed quite good agreement with the measured temperatures. The model estimations are close to the observed data, especially under the boundary layer where the higher concentrations are observed. This is important, since in dispersion simulations the higher concentrations are most significant. Problems with concentration overestimations appears as the height from the ground increase and especially over the boundary layer height. The dispersion of the scalar seems to be underestimated resulting in greater concentrations (temperature). One possible reason for this could be the fact that model simulations were performed using “one step” mean wind velocity profile, which was estimated for the whole time of the experiment. This means that structures in the wind flow, as the von Karman vortices, could not be described as an input to the model. This information is of great importance since the pollutants can be trapped in such structures and carried away at the upper parts of the interaction zone, resulting in this way in larger spread of the pollutant and thus smaller concentrations. Another important parameter is that as the height increases the energy dissipation rate (ε) decrease, causing smaller fluctuations and consequently smaller dispersion. The corrected modeling of the energy dissipation rate should be examined, at cases of dispersion over the boundary layer.

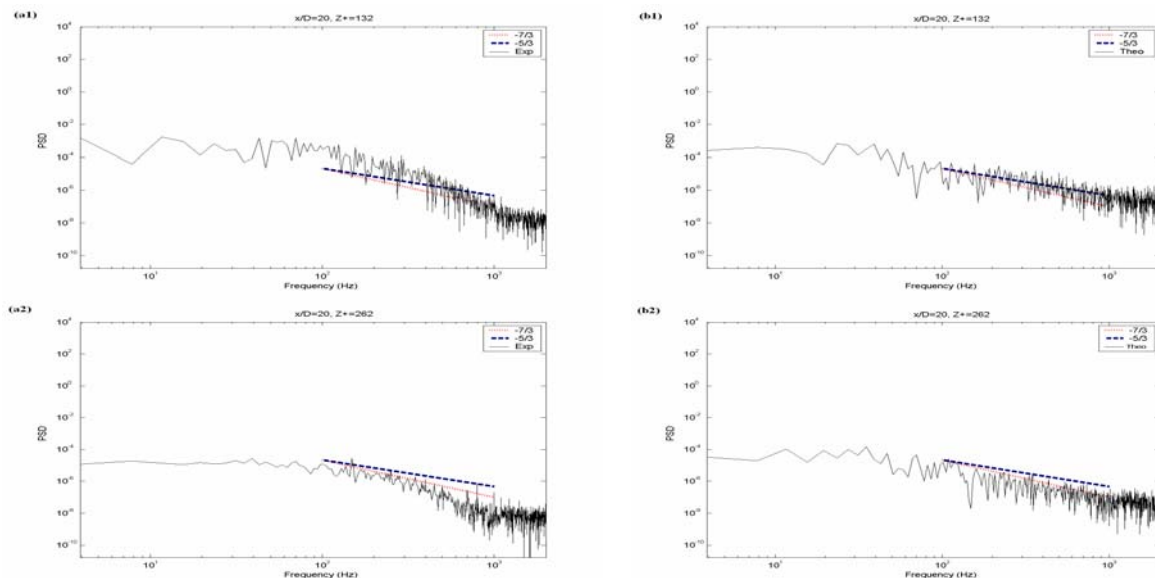


Figure 5. Power Spectra Density plots of experimental (a) and predicted (b) concentrations at $x/D=20$ and normalized heights $Z+=132$ (1), 262 (2)

The power spectra analysis showed that the observed temperature field deviates for the $-5/3$ power law, exhibiting regions of other slopes, such as $-7/3$. The analysis of the simulated data showed that the model prediction exhibit similar behaviour, but with differences in the number of regions and in their width. The calculation of the Lagrangian particle velocity PDF's presents the close relation between the concentration predictions and the particle velocity distribution. When the model correctly reproduces the wind velocity distribution, the dispersion calculations lead to correct concentration fields. For this reason, further development must be done in order to improve the PDF that the model exhibits, especially at areas of low particle concentration, as the upper parts of the boundary layer and over it.

REFERENCES

- Davakis, E., S. Andronopoulos, J.G. Bartzis and S.G. Nychas*, 2004: Validation study of the Lagrangian dispersion particle model Dipcot over complex topographies using different concentration calculation, *Int. J. of Environment and Pollution*, 20, Nos 1-6, 33-46.
- Franzese, P., A.K. Luhar, M.S. Borgas* 1999: An efficient Lagrangian stochastic model of vertical dispersion in the convective boundary layer, *Atmospheric Environment*, 33, 2337 – 2345.
- Rodean C.H.*, 1994: Notes of the Langevin model for turbulent diffusion of “Marked” Particles, Lawrence Livermore National Laboratory, US.
- Sideridis, G.A., E.G. Kastrinakis, S.G. Nychas*, 1998: Turbulent heat flux measurements in a quasi-two-dimensional flow and in presence of large scale structures, *Progress in Astronautics and Aeronautics*, 182, 255-269.
- Sideridis, G.A., E.G. Kastrinakis, S.G. Nychas, S.G.*, 1999: Conditional analysis of turbulent heat transport in a quasi two dimension wake interacting with the boundary layer, *Inter. J. of Heat and Mass Transfer*, 42, 3481-3494.
- Sideridis, G.A., E.G. Kastrinakis, S.G. Nychas*, 2002: Scalar transport in a quasi-two-dimensional turbulent wake interacting with a boundary layer, *Inter. J. of Heat and Mass Transfer*, 45, 1965-1982.
- Thomson, D.J.*, 1987: Criteria for the selection of stochastic models of particle trajectories in turbulent flows, *J. Fluid Mechanics*, 180, 529-556.
- Wilson, D. J., B.L. Sawford*, 1996: Review of Lagrangian stochastic models for trajectories in the turbulent atmosphere, *Boundary Layer Meteorology*, 78, 191-210.